

Electronic heat transport for a multiband superconducting gap in Sr_2RuO_4

P.L. Contreras

*Departamento de Física, Universidad De Los Andes,
Mérida, 5101, Venezuela.*

Recibido el 16 de noviembre de 2010; aceptado el 9 de agosto de 2011

This paper gives a detailed numerical study of the superconducting electronic heat transport in the unconventional multiband superconductor Strontium Ruthenate Sr_2RuO_4 . The study demonstrates that a model with different nodal structures on different sheets of the Fermi surface is able to describe quantitatively experimental heat transport data. The contribution of the density of states DOS is given for each sheet of the Fermi surface and the total contribution is also calculated. Finally, a discussion of the universal character of the electronic heat transport in unconventional superconductors and its relation to the DOS based on the type of nodal structure of the superconducting gap in Sr_2RuO_4 is given.

Keywords: Electronic heat transport; unconventional superconductors; gap structure; superconducting density of states; line nodes; point nodes.

En este trabajo se presenta un estudio numérico detallado de la termoconductividad electrónica en el superconductor no convencional Rutinato de Estroncio Sr_2RuO_4 . Se muestra que un modelo con diferentes estructuras nodales en diferentes láminas de la superficie de Fermi es capaz de describir cuantitativamente datos de transporte térmico obtenidos experimentalmente. La densidad de estados se calcula para cada lámina de Fermi y se presenta su contribución total. Por último, se discute el carácter universal de la termoconductividad electrónica en los superconductores no convencionales con diferentes estructuras nodales en la brecha superconductora como es el compuesto Sr_2RuO_4 .

Descriptores: Termoconductividad electrónica; superconductores no convencionales; estructura de la brecha; densidad de estados superconductora; nodos puntuales; líneas de nodos.

PACS: 74.20.Rp; 74.70.Pq; 74.25.F-; 74.25.fc

1. Introduction

It is believed that Sr_2RuO_4 , a multiband superconductor with a Fermi surface composed of three sheets, (called the α , β and γ sheets), is an unconventional superconductor with some kind of nodes in the superconducting gap [1,2]. For instance, a number of theoretical works [3-7] have predicted the existence of line nodes on two of three sheets of the Fermi surface (α and the β sheets). While, many authors take the γ sheet to be nodeless, these works have been able to provide an agreement with the specific heat $C(T)$ [8,9], electronic heat transport experiments $\kappa(T)$ [10], and recently with ultrasound measurements $\alpha(T)$ as well. However, the existence of a nodeless gap for the γ sheet contradicts the nodal activity observed in ultrasound measurements below T_c in Sr_2RuO_4 [11]. Firstly, the anisotropy inherent to the \mathbf{k} dependence of electron-phonon interaction shows that γ sheet dominates ultrasound attenuation for L[100], L[110], and T[110] sound modes. Secondly, these modes show very similar temperature power law behavior below T_c ; therefore the γ sheet should also have a similar nodal structure.

The sound attenuation $\alpha(T)$ in Sr_2RuO_4 can distinguish the nodal structure of the γ sheet from that one of the α and β sheets. In contrast, electronic thermal conductivity and specific heat have an integral effect (the three sheets contribute to $\kappa(T)$ and $C(T)$), and it is very difficult to discern if the order parameter in each of the Fermi sheets has similar nodal structure. So far, to summarize there is a considerable consensus

as to the unconventional behavior [1,2,13], and the symmetry of the superconducting gap [14], and probably also, to the multiband nature of the superconducting state, nevertheless certainly there is as yet no agreement as to the nodal structure of the superconducting gap on the different sheets of the Fermi surface.

It has been proposed a model based on symmetry considerations [12], which explains the temperature behavior of the ultrasound attenuation for the L[100], L[110], and T[110] sound modes. According to this model, the γ sheet should have well-defined point nodes, and the β and/or α bands could have also point nodes, but with an order of magnitude smaller than for the γ band and resembling lines of a very small gap. The purpose of this article is to apply, the model found in Ref. 12 to the study of the electronic heat transport of Sr_2RuO_4 .

Sr_2RuO_4 has a body centered tetragonal structure with a layered square-lattice structure similar to that of many high temperature copper-oxide superconductors [1]. The critical temperature T_c varies strongly with non magnetic impurity concentration, $T_c \approx 1.5$ K for pure samples. The normal state displays Fermi liquid behavior [2]. According to some authors [14,15] the symmetry of the gap structure is believed to be a time reversal broken state, with the symmetry transforming as the two dimensional irreducible representation E_{2u} of the tetragonal point group D_{4h} . Additionally in Ref. 17 the order parameter of Sr_2RuO_4 was proposed according to a novel mechanism due to antiferromagnetic fluctuations.

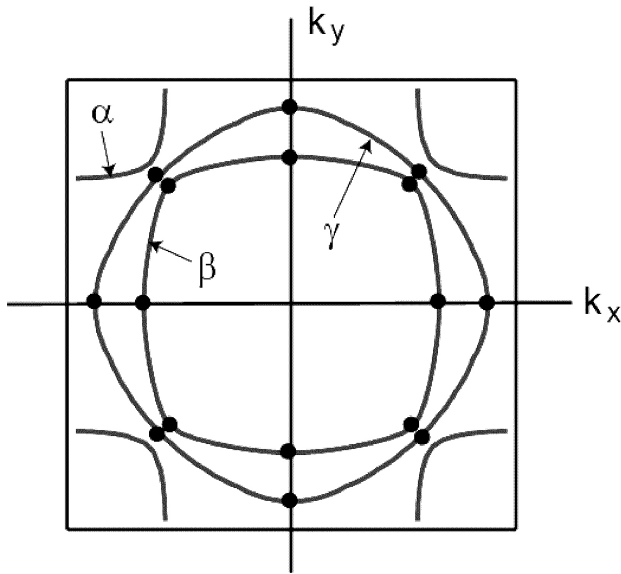


FIGURE 1. The black dots show the positions of the point nodes in the superconducting gap on the β and γ Fermi surface sheets in Sr_2RuO_4 , as determined by Eqs. 2 and 3. Each solid circle represents two nodes, at positions $\pm k_z$.

2. Model for the superconducting gap structure

As I mentioned before, the gap model proposed in Ref. 12 is extended here for the study of the electronic heat transport. The assumption of a superconducting order parameter according to symmetry considerations, where

$$\Delta_{\mathbf{k}} = (\mathbf{d}^i(\mathbf{k}) \cdot \mathbf{d}^{i,*}(\mathbf{k})) \Delta^i(T),$$

with different $\mathbf{d}^i(\mathbf{k})$ - vector order parameters for different i -Fermi sheets, transforming according to the two dimensional irreducible representation E_{2u} of the tetragonal point group D_{4h} , it yields the form

$$\mathbf{d}^i(\mathbf{k}) = \mathbf{e}_z [d_x^i(\mathbf{k}) + i d_y^i(\mathbf{k})]; \tag{1}$$

where the explicit expressions I use for d_x^i and d_y^i are

$$d_x^i(\mathbf{k}) = \delta^i \sin(k_x a) + \sin\left(\frac{k_x a}{2}\right) \cos\left(\frac{k_y a}{2}\right) \cos\left(\frac{k_z c}{2}\right), \tag{2}$$

and

$$d_y^i(\mathbf{k}) = \delta^i \sin(k_y a) + \cos\left(\frac{k_x a}{2}\right) \sin\left(\frac{k_y a}{2}\right) \cos\left(\frac{k_z c}{2}\right), \tag{3}$$

with d_x^i and d_y^i real. The factors δ^i were obtained in Ref. 12 by fitting experimental data on ultrasound attenuation of Ref. 11.

For this model, the nodal structure of the γ band predicts eight symmetry-related nodes for \mathbf{k} , lying on the symmetry equivalent $\{100\}$ planes (see Fig. 1) and also eight symmetry-related nodes in $\{110\}$ planes for the γ sheet as well. The

nodal structure of the order parameter for the β and/or α sheets yields to eight symmetry-related nodes for \mathbf{k} , lying on the symmetry equivalent $\{100\}$ planes (see also Fig. 1) and also eight symmetry-related nodes in $\{110\}$ planes. All point nodes are ‘‘accidental’’ in the sense that they are not required by symmetry, but exist only if the material parameters δ^γ and $\delta^{\beta/\alpha}$ have values in a certain range.

3. Electronic heat transport

In order to calculate the electronic heat transport or thermal conductivity for an unconventional superconductor, a standard formalism previously reported [19] is extended here to account for tight binding effects. For this purpose, the incorporation of tight binding effects for the nodal structure and the Fermi surface is the most important. A self-consistent calculation of the gap function and of the energy-dependent impurity scattering rate is beyond the scope of this article, this leads to the approximation where the interband scattering effects are totally neglected.

Recent induced impurity scattering measurements [23] of the thermal conductivity for temperatures close to 100 mK, have shown a remarkably universal character of the electronic heat transport in Sr_2RuO_4 . It has been suggested [23] that Sr_2RuO_4 is in the unitary impurity scattering regime. In addition to this, some time ago it was suggested the idea [21] that the transport properties of heavy-fermion superconductors can be explained in terms of an effective electron scattering rate which, except for the lowest temperatures is approximate temperature independent and equal in magnitude to that of the normal state. Such a lifetime arises in a self-consistent treatment of impurity scattering near the strong regime.

Thus, in the proposed not self-consistent treatment, we take the impurity scattering superconducting quasiparticle lifetime τ_n^i to be equal to the impurity scattering predicted for the unitary limit in the normal state.

$$\frac{1}{\tau_n^i} = \frac{n_i}{\pi N_0^i U_0}. \tag{4}$$

N_0^i is the density of states for the i -sheet at the Fermi level, and the strength of the impurity potential $U_0^i \gg 1$.

The energy of a normal-state i -sheet $\epsilon_{\mathbf{k}}^i$ is the same as the value previously reported [12]. The tight binding parameters used for the γ sheet are

$$(E_0 - E_F, t, t') = (-0.4, -0.4, -0.12).$$

These values are in agreement with Haas-Van Alfen, and ARPES experiments [16,17]. The calculation of the thermal transport makes use of the Fermi velocity as determined from the expression for the band structure; however, a calculation with the unit isotropic vector of the Fermi velocity $\hat{\mathbf{v}}_{F,j} = (\hat{\mathbf{j}} \cdot \mathbf{k}_i)$ provides the same result.

The expression used to calculate the electronic heat transport due to non magnetic impurity scattering in unconventional superconductors is validated for energies $\epsilon \sim T$ and

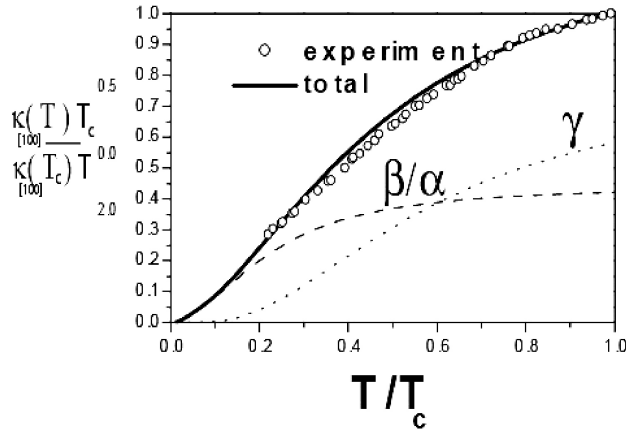


FIGURE 2. Numerical fit of the in-plane thermal conductivity components [100] normalized at T_c . Experimental data is taken from [10].

low impurity concentrations. A suitable equation to compare numerical calculations with experiments is given by

$$\frac{\kappa_j(T)}{\kappa_j(T_c)} = \frac{I}{T} \sum_i \int_0^\infty d\epsilon \epsilon \left(-\frac{\partial f}{\partial \epsilon} \right) A_j^i(\epsilon), \quad (5)$$

here the constant $I = 6/(\pi^2 T_c)$, j refers to one of the two basal directions [100] and [110] and i labels the sheets on the Fermi surface. $A_j^i(\epsilon)$ is given by

$$A_j^i(\epsilon) = \frac{\langle \hat{v}_{F,j}^{i,2}(\mathbf{k}) \text{Re} \sqrt{\epsilon^2 - |\Delta_{\mathbf{k}}^i|^2} \rangle_{FS}}{\sum_i \langle \hat{v}_{F,j}^{i,2}(\mathbf{k}) \rangle_{FS}}. \quad (6)$$

The gap $\Delta_{\mathbf{k}}^i$ corresponds to the expressions for d_x^i and d_y^i given in Eqs. 2 and 3. $\hat{v}_{F,j}^{i,2}$ are the unit Fermi velocity vectors for each sheet. In this equation vertex corrections have been neglected, since we have not carried out a self-consistent evaluation of the order parameter. It is assumed a temperature dependence of the form $\Delta^i(T) = \Delta_0^i \sqrt{1 - (T/T_c)^3}$, which is sometimes used in the literature [6].

Figure 2 shows the numerical results for the temperature dependence of the normalized electronic heat transport calculated by evaluating Eq. 5. The experimental results are from Ref. 10. The obtained fittings are: $\Delta_0^\beta \approx 0.09$ meV, and $\Delta_0^\gamma \approx 0.3$ meV.

The numerical calculation of the electronic thermal conductivity for the basal [100] direction is shown in Fig. 2. The total κ gives an excellent agreement with the experimental data. This experimental data is for pure samples with $T_c \approx 1.44$ K. Contributions from each band are also calculated. Figure 2 shows that lines of very small point gaps on the β and/or α sheets could dominate the behavior of the electronic thermal conductivity at low temperatures. On the other hand, point nodes on the γ sheet give an insignificant contribution at low temperatures. This shows in principle that the electronic thermal conductivity in Sr₂RuO₄ is an integral effect where, in contrast to sound attenuation, the contributions

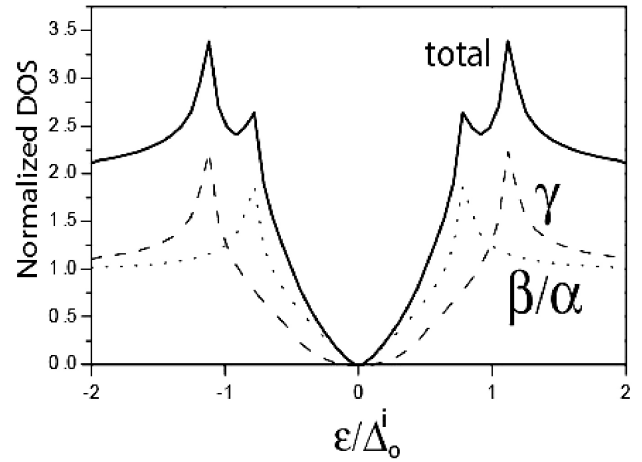


FIGURE 3. Numerical calculations of the superconducting density of states DOS for the β and γ sheets according to our model.

for all the bands are needed in order to explain the experimental data.

It is important to notice that although the nodes in the proposed model are both point nodes, the low temperature properties of the nodal structure for the β and/or α sheets have some of the properties of line nodes, as there is a very low gap along the line joining the nodes. Hence, the result match the one provided by horizontal line nodes as is the case of the Zhitomirsky-Rice model [3]. However the fit in Fig. 2 provides in principle, a strong support for the essential features of the order parameter symmetry model of Ref. 12.

Due to the importance of anisotropy tight binding effects, I also consider worth to calculate κ for the [110] direction, finding that there are no crucial differences between the calculation for any of the two directions; even in the case when anisotropic effects are included. This proves that the $\kappa(T)$ dependence on T (in contrast to the sound attenuation) is in overall equally dominated from contributions coming from all the sheets and explains the apparent line nodes behavior of κ where the β and α sheets give a major contribution.

4. Density of states and universal behavior of the electronic heat transport

Next, I attempt to give a qualitative analysis of the universal behavior of the superconducting electronic thermal conductivity according to this model. First, a numerical calculation of the density of states DOS in the superconducting state of the γ and β sheets is performed. The numerical calculation of the DOS is made with the equation

$$N(\epsilon) = N_0^i \text{Re} \left\langle \frac{\epsilon}{\sqrt{\epsilon^2 - |\Delta_{\mathbf{k}}^i|^2}} \right\rangle_{FS}, \quad (7)$$

N_0^i is the DOS at the Fermi level for each band, and the gap Δ_0^i corresponds to the one given by the expressions for d_x^i and d_y^i . For the purpose of finding the energy dependence of the DOS the previous expression is calculated at $T = 0$.

The numerical calculation of the DOS is shown in Fig. 3. For the β and γ sheets Fig. 3 shows that for the low energy Bogoliubov excitations the DOS in the β sheet behaves linearly in energy, as it is predicted for line nodes. On the other hand, the γ band shows a quadratic behavior in energy, as it is expected for a superconducting DOS with point nodes. Also from Fig. 3 it can be noticed that the zero temperature gap amplitude for the γ band is larger than the one for the β band.

In order to elucidate the universal behavior in κ from the symmetry model, an intuitive approach which was found to be successful in Ref. 20 will be used below. It is noticed that a more general theoretical analysis as the one developed for the universal behavior of the sound attenuation in Ref. 18 can be performed easily here. I show that it is possible to provide the main results in the case of a multiband superconductor. I start with a simple expression for the expected low energy dependence of the DOS where the nodal points (the points where the Bogoliubov quasiparticle's energy is zero) determine the low temperature thermodynamic properties.

As it was noticed previously, the largest material parameter δ^γ gives rise to a well defined point-nodes topology for the order parameter in the γ band, therefore as shown in Fig. 3, a qualitative behavior of the DOS yields the following expression for the density of states of the γ -sheet

$$\frac{N^{s,\gamma}}{N_0^\gamma} \simeq \frac{\epsilon^2}{\Delta_0^{\gamma,2}}. \quad (8)$$

On the other hand, the material parameter δ^β gives rise to a line of very small point nodes on the β sheet and it can be approximated by the following expression

$$\frac{N^{s,\beta}}{N_0^\beta} \simeq \frac{\epsilon}{\Delta_0^\beta}, \quad (9)$$

where Δ_0^γ and Δ_0^β are the maximum gaps for each Fermi sheet.

Close to the strong scattering regime and approaching the universal limit, I generalize the results of Ref. 20 to the case of a two gaps superconductor. In Ref. 20 it is supposed that the low lying Bogoliubov excitations acquire an imaginary part $\epsilon \rightarrow \epsilon + i\Gamma$. These excitations possesses an energy independent life time $\tau = 1/2\Gamma$ and because of the energy uncertainty principle, the low energy quasiparticles have a spread in energy of the order of Γ which is called the zero energy scattering rate [18].

Therefore, close to the unitary limit the DOS for both sheets is given by

$$\frac{N^{s,\gamma}}{N_0^\gamma} \simeq \frac{\Gamma_\gamma^2}{\Delta_0^{\gamma,2}}, \quad (10)$$

and

$$\frac{N^{s,\beta}}{N_0^\beta} \simeq \frac{\Gamma_\beta}{\Delta_0^\beta}, \quad (11)$$

where Γ_γ and Γ_β are the spreads in energy for the γ and β sheets.

The low temperature specific heat c_V associate with the constant DOS at low energies and temperatures $T \leq \Gamma$ and for both sheets is given according to [20] by

$$c_V = c_V^\gamma + c_V^\beta \simeq \frac{2\pi^2}{3} k_B^2 T \left[N_0^\gamma \frac{\Gamma_\gamma^2}{\Delta_\gamma^2} + N_0^\beta \frac{\Gamma_\beta}{\Delta_\beta} \right]. \quad (12)$$

where k_B is the Boltzmann constant. This way a simple estimate of the bulk electronic thermal conductivity at low energies and for both sheets in the limit of the universal behavior (at temperatures $T \leq \Gamma$) is given by the generalization of equation in Ref. 20

$$\kappa = \kappa^\gamma + \kappa^\beta \simeq c_V^\gamma v_{F,\gamma} l_\gamma + c_V^\beta v_{F,\beta} l_\beta, \quad (13)$$

with

$$l_\gamma = v_{F,\gamma} \frac{\hbar}{\Gamma_\gamma}$$

and

$$l_\beta = v_{F,\beta} \frac{\hbar}{\Gamma_\beta}$$

the mean free paths for both sheets. Finally, I found the electronic heat transport in the limit of the universal behavior to be

$$\frac{\kappa}{T} \approx \frac{\pi^2 \hbar k_B^2}{3} \left[v_{F,\beta}^2 \frac{N_0^\beta}{\Delta_0^\beta} + v_{F,\gamma}^2 \left(\frac{N_0^\gamma \Gamma_\gamma}{\Delta_0^{\gamma,2}} \right) \right]. \quad (14)$$

A numerical evaluation of the previous equation can be performed by using the values for the Fermi velocities $v_{F,\beta} = 95.9$ Km/seg and $v_{F,\gamma} = 59.5$ Km/seg according to [2], the values for Δ_0^γ and Δ_0^β given previously in this paper, and the values of the DOS at the Fermi level of Ref. 2. For the spread in energy in the unitary limit, I take a very simple approximation $\Gamma_\gamma \sim \Delta_0^\gamma$ following the appendix of Ref. 18.

Therefore, I find the bulk thermal conductivity for this two sheets model approximately equal to

$$\kappa_{\text{theoretical}}/T \approx 0.8 \text{ W/K}^2 \text{ m}$$

and which is lower than the experimental value found in Ref. 23 of

$$\kappa_{\text{experimental}}/T \approx 1.7 \text{ W/K}^2 \text{ m}.$$

5. Final remarks

It is found that with two different gap structures characterized in the γ , β and/or α sheets by point nodes of different magnitude, the calculation of the temperature behavior of the superconducting electronic heat transport $\kappa(T)$ leads to an excellent agreement with the existent experimental data [22]. These results also show that in contrast to the ultrasound attenuation $\alpha(T)$, which is able to identify different nodal structures in different bands, there is not relevant anisotropy for the quantities $\kappa_{[100]}$ and $\kappa_{[110]}$. This makes difficult to

identify the nodal structure in Sr₂RuO₄ from electronic thermal conductivity data. Finally, the numerical calculation of the DOS for each sheet, allows us to qualitatively estimate the value of the universal limit for the electronic heat transport to be lower than the value observed experimentally in Ref. 23.

Acknowledgments

I thank Dr. M. Tanatar for stimulating discussions and for providing the experimental data in Fig. 2. I also acknowl-

edge discussions with Prof. Michael Walker from the University of Toronto, Prof. José Rodríguez at SUPERCOM from la Universidad de Carabobo, and Prof. Rodrigo Casanova. This research was supported by the Grant CDCHTA number C-1479-07-05-AA.

-
1. Y. Maeno *et al.*, *Nature* **372** (1994) 532.
 2. A. Mackenzie and Y. Maeno, *Rev. of Modern Physics* **75** (2003) 657.
 3. M. Zhitomirsky and T. M. Rice, *Phys. Rev. Lett.* **87** (2001) 057001.
 4. D. Agterberg, T. M. Rice, and M. Sigrist, *Phys. Rev. Lett.* **78** (1997) 3374.
 5. M. J. Graf and A. V. Balatsky, *Phys. Rev. B* **62** (2000) 9697.
 6. W. C. Wu and R. Joynt, *Phys. Rev. B* **65** (2002) 104502-1.
 7. K. I. Wysokiński, G. Litak, J. F. Annett, and B. L. Györfy, *Phys. Stat. Sol (b)* **236** (2003) 325.
 8. Y. Hasegawa, K. Machida, and M. Ozaki, *J. Phys. Soc. Jpn.* **69** (2000) 336.
 9. K. Deguchi, Z. Q. Mao, H. Yaguchi, and Y. Maeno, *Phys. Rev. Lett.* **92** (2000) 047002-1-4.
 10. M. Tanatar, S. Nagai, Z. Q. Mao, Y. Maeno, and T. Ishiguro, *Phys. Rev. B* **63** (2001) 064505.
 11. C. Lupien, W. A. MacFarlane, C. Proust, L. Taillefer, Z. Q. Mao, and Y. Maeno, *Phys. Rev. Lett.* **86** (2001) 5986.
 12. P. Contreras, M. Walker, and K. Samokhin, *Phys. Rev. B* **70** (2004) 184528.
 13. T. M. Rice and M. Sigrist, *J. Phys. Condens. Matter* **7** (1995) L643.
 14. G. M. Luke *et al.*, *Nature* **394**, (1998) 558.
 15. M. Walker and P. Contreras, *Phys. Rev. B* **66** (2002) 214508.
 16. C. Bergemann, A. P. Mackenzie, S. R. Julian, D. Forsythe, and E. Omichi, *Adv. Phys.* **53** (2003) 639.
 17. I.I. Mazin and D. J. Singh, *Phys. Rev. Lett.* **79** (1997) 733.
 18. M. Walker, M. Smith, and K. Samokhin, *Phys. Rev. B* **65** (2002) 014517.
 19. V. P. Mineev and K. V. Samokhin, *Introduction to Unconventional Superconductivity* (Gordon and Breach, Amsterdam, 1999).
 20. M. Zhitomirsky and M. Walker, *Phys. Rev. B* **57** (1998) 8560.
 21. S. Schmitt-Rink, K. Miyake, and C. M. Varma, *Phys. Rev. Lett.* **57** (1986) 2575.
 22. M. Tanatar, M. Suzuki, S. Nagai, Z. Q. Mao, Y. Maeno, and T. Ishiguro, *Phys. Rev. Lett.* **86** (2001) 2649.
 23. M. Suzuki, M. Tanatar, N. Kikugawa, Z. Q. Mao, Y. Maeno, and T. Ishiguro, *Phys. Rev. Lett.* **88** (2002) 227004.